JOURNAL OF PHARMACEUTICAL SCIENCES

OCTOBER 1981
VOLUME 70 NUMBER 10

RESEARCH ARTICLES

Solid-State Decomposition of Alkoxyfuroic Acids

J. T. CARSTENSEN *x and ROHIT KOTHARI ‡

Received November 10, 1980, from the **School of Pharmacy, University of Wisconsin, Madison, WI 53706*, and ‡*Ryker Laboratories, St. Paul, MN 55100.* Accepted for publication March 6, 1981.

Abstract □ A series of alkoxyfuroic acids with alkyl lengths of n = 8–18 was synthesized, and the solid-state decomposition was studied. Bawn kinetics were adhered to, and the solid and liquid decomposition rate constants were established; they followed an Arrhenius relationship well, with energy of activations and preexponential factors being a function of the chain length. There was a break in this correlation between n = 14 and n = 16. The liquefaction points were of the expected correlation with inverse temperature. The isokinetic temperature (T_i) fell fairly well on the line demonstrated for other compound series.

Keyphrases □ Solid-state decomposition—alkoxyfuroic acids with alkyl chain lengths of n = 8–18 □ Alkoxyfuroic acids—Arrhenius relationship, energy of activation and preexponential factors as a function of chain length □ Bawn kinetics—solid and liquid decomposition rate constants of alkoxyfuroic acids

Chemical decomposition of pure solids has been discussed sporadically in the literature, the principal publications being those of Prout and Tompkins (1) and Bawn (2). The reactions are usually dictated to a great extent by physical (*e.g.*, active site propagation) rather than chemical steps, resulting in high activation energies (300–400 kJ) when the reaction is one where:

$$\text{solid} \rightarrow \text{solid} + \text{gas}$$

Scheme I

This reaction (Scheme I) was essentially covered by Prout and Tompkins, whereas the reaction (Scheme II) treated by Bawn is:

$$\text{solid} \rightarrow \text{liquid} + \text{gas}$$

Scheme II

Several reactions of this latter type were reported in the pharmaceutical literature (3–6). In these reactions (Scheme II), it was shown that the part occurring in the solid is not necessarily dictated by active site propagation and that chemical factors are much more prevalent (5) than when Scheme I applies. Chemical substituent effects have, for instance, been demonstrated (3–5).

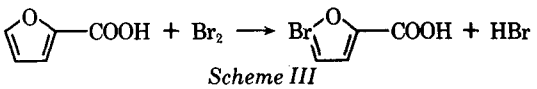

Scheme III

The work described in this report deals with chemical substituent (chain length) effects in a series of alkyloxyfuroic acids. One of these acids (7) was previously shown to be a hypolipidemic agent.

EXPERIMENTAL

Synthesis—The compounds studied were 5-alkyloxy-2-furoic acids, *i.e.*, RCOOH, where R = C_nH_{2n+1}–O–(C_4H_2O)– and where n = 8, 10, 12, 14, 16, and 18. The syntheses were carried out by the method described by Parker *et al.* (7) with a few modifications. Furoic acid was first brominated to give 5-bromofuroic acid, using carbon tetrachloride as a solvent (Scheme III).

A 2-liter round-bottom flask, fitted with a reflux condenser, drying tube, and magnetic stirrer, was charged with 250 g of furoic acid and 1.2 liters of carbon tetrachloride. The mixture was stirred until all of the furoic acid was dissolved. The solution was heated to 40°, and then 500 g of bromine was added slowly through a funnel directly fitted to the flask. The reaction mixture was then refluxed on a water bath for 5 hr. At the end of the refluxing period, carbon tetrachloride was distilled off.

The product of the reaction was dissolved in boiling water and filtered hot. Upon cooling, the bromosubstituted acid precipitated. It was further purified by recrystallization from hot water. To eliminate any dibromofuroic acid that might have formed, the barium salt was prepared as follows. For each gram of the product, 25 cm^3 of water was added and made strongly alkaline with ammonium hydroxide; 1 g of barium chloride was added with some activated charcoal. After 15 min, the solution was filtered. The filtrate was acidified with hydrochloric acid; the 5-bromofuroic acid, which precipitated out, was recrystallized from hot water. The yield was 60%, mp 186°, in agreement with the melting point obtained by Whittaker (8).

The 5-alkyloxy-2-furoic acid was next synthesized from the bromofuroic acid in two stages as shown in Schemes IV and V.

A reaction flask was charged with 1 liter of toluene, and ~0.1 liter of the solvent was distilled off to dry. The toluene remaining was cooled to 40° under nitrogen, and 0.33 mole of n-alkanol and 0.45 mole of sodium hydride (as a 50% dispersion in oil) were added. The mixture was refluxed

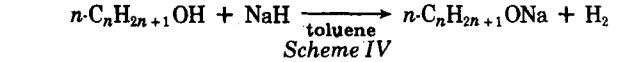

Scheme IV

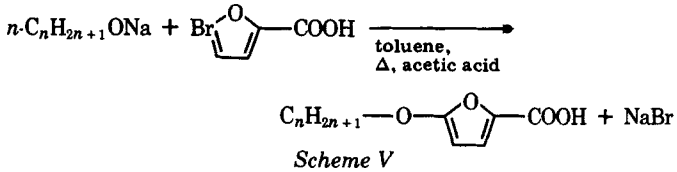

Scheme V

0022-3549/81/1000-1095$01.00/0

Table I—Properties of 5-Alkyloxy-2-furoic Acids

n[a]	Melting Point	Heat of Fusion, ΔH_f, Obtained from Kinetic Data, kJ/mole	ΔH_{DTA} from Thermal Analysis, kJ/mole	$q = \Delta H_f - \Delta H_{DTA}$, kJ/mole	Density, g/cm^3 [b]	Crude Yield, %	Recrystallized Yield, %
8	127°	111	29	82	1.28	60	47
10	125°	53	—[c]	—[c]	1.23	40	30
12	122°	72	41.2	31	1.13	72	63
14	119°	68	31.6	36	1.13	72	63
16	118°	63	—[c]	—[c]	1.11	35	23
18	117°	73	36	37	—	58	50
5-BFA[d]	186°					75	70

[a] n = alkyl length. [b] Densities done by pycnometry. In the case of n = 18, the material wets very poorly in solvents in which it is poorly soluble and density data are not available. [c] Decomposition pertubates thermogram too much in these cases to draw conclusions. [d] 5-Bromofuroic acid.

for 3 hr and then cooled under nitrogen to 40–45°. A suspension of 0.2 mole of 5-bromofuroic acid in 0.2 liter of dry toluene was added rapidly. The reaction mixture was held at 60° for ~1 hr to ensure that the balance of the sodium hydride had reacted to form the sodium salt of the acid. It was then heated at reflux temperature for 16 hr.

The mixture was cooled to 30°, and 1.2 liters of ether was added, followed by 0.3 liter of 15% acetic acid. Stirring was continued for ~30 min. The organic portion was separated with the help of a separator and then was washed three times with either distilled water or saturated sodium chloride solution. The solution was dried with calcium chloride, and then the drying agent was removed by vacuum filtration. Most of the ether was stripped off with the help of a flask-evaporator and a hot water bath held at 45°. The concentrated solution was chilled in a freezer for 12–15 hr.

The precipitated solid was filtered off and washed with cold toluene. The crude product was dissolved in hot 2-butanone or acetone, and then activated charcoal was added. The mixture was stirred for a few minutes and filtered while hot. This solution was cooled gradually to 5°, and the recrystallized product was filtered off after a few hours. Recrystallization was carried out at least three times to ensure purity. The compounds were identified with the help of NMR and mass spectra and, where possible, differential scanning calorimetry. Melting points were determined and are listed in Table I.

Kinetic Studies—Kinetic studies were carried out by preparing a sample *in vacuo* in a sample bulb with an attached mercury manometer such as was described previously (3, 6). The whole assembly was placed in a tall thermostatically controlled bath with either water or mineral oil as the medium; temperature control was ±0.2°. The amount of gas pressure at any time can be deduced from a knowledge of the volume, mercury height, and density of mercury at the temperature in question and can then be converted to number of moles of gas produced.

Condensation characteristics and mass spectra of the gas confirmed it to be carbon dioxide. Since, in the manner described, the decomposition takes place in a system that is evacuated but that contains mercury vapor in the headspace, several control studies were done in break-seal tubes (3) to ascertain that the mercury vapor did not affect reaction rates.

Vapor Pressure Studies—Since the possibility exists that the decomposition of a solid at constant volume occurs in the vapor phase, the vapor pressure of the various solids was determined. The Knudsen effusion method was used (9–12). In this method, the rate of vapor loss through a small orifice is measured gravimetrically under conditions of free molecular flow; the vapor pressure is calculated directly from the proportionality between the rate of mass loss and the vapor pressure.

The Knudsen cells used were aluminum crucibles with a lid placed on the top in conjunction with an "O" ring. A small orifice (0.5-mm diameter) was drilled in the lid. The mean value of the orifice diameter was determined microscopically. The fidelity of the method was checked by determining vapor pressures of a compound (benzoic acid) with well-established vapor pressure values (13). The cells were placed on the pan of an electrobalance in a vacuum chamber such as was described previously (14).

To determine the decomposition rate constant in the vapor phase, a 2-liter bulb was equipped with a break-seal tube. The amount of alkoxyfuroic acid necessary to (just) saturate the bulb at 95° was calculated from the vapor pressure *versus* temperature curve. This amount was then added to the bulb as a methanol solution. The solvent was then evaporated off (on the vacuum rack) at room temperature, and the nonbreak-seal end was fused off. The bulb was placed at 95°, and the amount of carbon dioxide evolved after 1 week was determined, in this case by means of a McLeod gauge with a 1:10,000 ratio of compression capacity.

RESULTS AND DISCUSSION

The general pattern is that the solid decomposes by some means and that a liquid decomposition product is formed. There are three main feasible models that could account for this reaction.

In Model A, the solid (RCOOH) evaporates and decomposes in the vapor phase to RH and CO_2, and RH condenses. Decomposition in the solid state is negligible.

In Model B, the solid (RCOOH) decomposes in the solid state and, in addition to carbon dioxide, forms liquid RH in which RCOOH is insoluble. [Prout–Tompkins kinetics (1)].

In Model C, the solid (RCOOH) decomposes in the solid state and, in addition to carbon dioxide, forms liquid RH in which RCOOH is soluble [Bawn kinetics (2)].

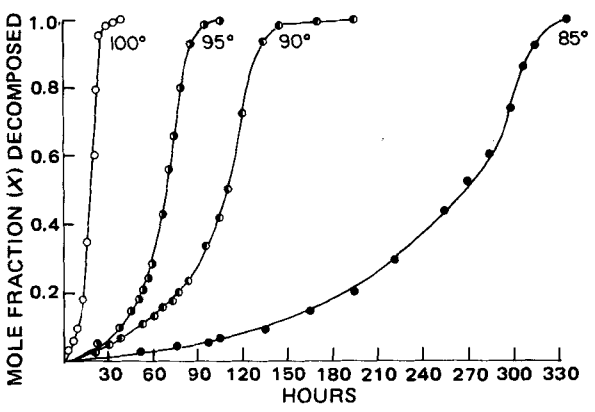

Figure 1—*Decomposition of octyloxy furanoic acid at various temperatures. Key:* ●, *85°;* ◐, *90°,* ◑, *95°; and* ○, *100°.*

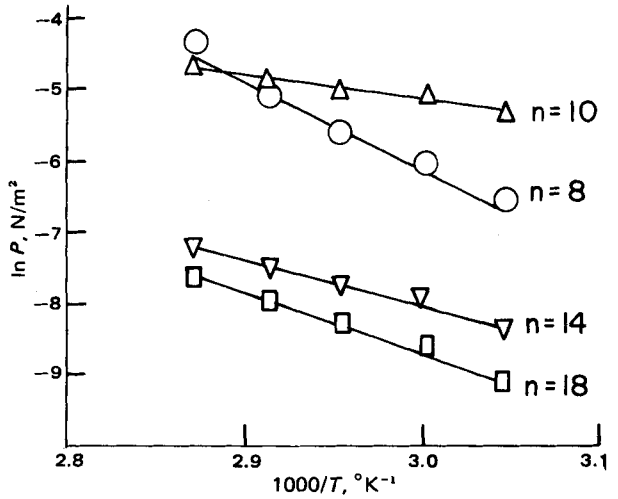

Figure 2—*Vapor pressures as a function of temperature. Only four of the alkoxyfuroic acids are plotted to avoid crowding. Key:* ○, n = *8;* △, n = *10;* ▽, n = *14; and* □, n = *18.*

Table II—Mole Fraction (X_s) at Complete Liquefaction

Temperature (T)	n[a]					
	8	10	12	14	16	18
127°	0	0				
125°			0			
119°				0		
118°					0	
117°						0
100°	0.60	0.59	0.56	0.48	0.65	0.70
95°	0.73	0.68	0.65	0.62	0.72	0.74
90°	0.84	0.75	0.76	0.76	0.80	0.80
85°	0.91	0.80	0.83	0.78	0.90	0.89
Eq. 8, N[b]	4	4	4	4	3[b]	4
Correlation coefficient	−0.997	−0.999	−0.997	−0.990	−0.994	−0.957
Slope	−13,355	−6360	−8655	−8117	−7580	−8824
Intercept	34.9	16.1	22.4	21.1	19.3	22.5
ΔH_f, kJ	111	53	72	68	63	73
T_0, °K	383	394	386	385	393	391
T_0, °C	110	121	113	112	120	118

[a] n = alkyl length. [b] Number of points used. In the case of n = 16, only the first 3 points were used since the point at 85° appears to be a (slight) outlier.

There is also the possibility of Model B or C in combination with Model A.

For Model A, Scheme VI applies:

$$\text{RCOOH(solid)} \rightarrow \text{RCOOH(vapor)} \rightarrow \text{RH} + \text{CO}_2$$

Scheme VI

If A denotes the amount of intact RCOOH, then by denoting its vapor pressure as P:

$$dA/dt = -k'P \qquad \text{(Eq. 1)}$$

Since P is simply a function of temperature, the reaction, carried out isothermally, would be zero order, with a rate constant of:

$$k_0 = k'P \qquad \text{(Eq. 2}a\text{)}$$

A typical decomposition curve is shown in Fig. 1. It is obvious from visual inspection that the decomposition is not zero order. Furthermore, the decomposition rate constants in the gas phase were found in the worst case (n = 8) to be of the order of 3×10^{-3} hr^{-1} at 95°. Vapor pressure curves are shown in Fig. 2. For n = 8, the pressure at 95° was 89×10^{-3} Pa ($\sim 9 \times 10^{-7}$ atm). The headspace (V) of the bulb/manometer was ~100 cm^3, so that (N denoting moles):

$$dN/dt = (V/RT)\, dP/dt = (V/RT)k'P \qquad \text{(Eq. 2}b\text{)}$$

which, with the previous figures, amounts to 0.9×10^{-11} mole/hr or (the molecular weight for n = 8 being 228) 2×10^{-6} mg/100 hr. Hence, Model A can be ruled out.

During the decomposition as time progresses, more and more liquid is present and less and less solid exists. At a particular point, no more solid is present and the entire sample is liquid. If Model B is correct, then this point should correspond to 100% decomposition. But this is not the case; this point occurs, on the average, at 75% decomposition. Hence, the parent compound (RCOOH) has a finite solubility, S moles/mole RH, and Model C seems to be a more feasible model. The mathematical consequences of the model are as follows (6). If X denotes mole fraction decomposed, if k_s is the decomposition rate constant of RCOOH in the solid state, and if k_l is the decomposition rate constant of RCOOH in solution in RH, then:

$$\ln(1 + AX) = \alpha t \qquad \text{(Eq. 3)}$$

where A is an adjustable parameter and t is time. The value of A is given by:

$$A = \alpha/k_s \qquad \text{(Eq. 4)}$$

and:

$$\alpha = k_l S - k_s S - k_s \qquad \text{(Eq. 5)}$$

S can be determined from the time, t_s, at which the system becomes completely liquid. If the amount decomposed at this point is X_s, then the amount not decomposed is $1 - X_s$ and, hence, the solubility is

$$S = (1 - X_s)/X_s \text{ moles/mole} \qquad \text{(Eq. 6)}$$

Beyond time t_s, the system is a solution and should adhere to first-order kinetics, *i.e.*:

$$\ln[(1 - X)/(1 - X_s)] = -k(t - t_s) \qquad \text{(Eq. 7)}$$

For Model C to apply, it is necessary that: (*a*) the data below time t_s can be linearized *via* Eq. 3; (*b*) the data above time t_s can be linearized by suitable liquid kinetic schemes; and (*c*) the value of k_l found from this latter scheme when inserted in Eq. 5, together with the solubility $S = (1 - X_s)/X_s$ and k_s from Eq. 4, gives a value of α in agreement with the value of α from Eq. 3. If the above statements hold, then a double check of the model is established for its correctness. Of course, a model is never

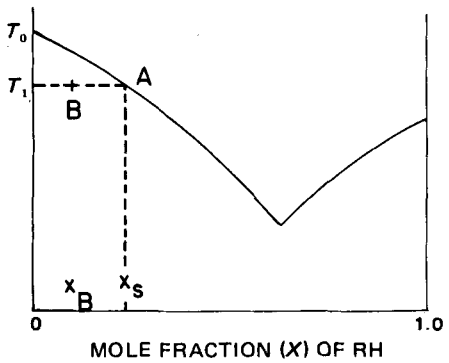

Figure 3—*Melting-point diagram of RCOOH and RH. If the decomposition is carried out at* T_1, *then at a certain time* (t_B) *a decomposition corresponding to* X_B *will have occurred. The amounts of solid and liquid will be determined by the weight arm rule. At a particular point in time* (t_s), *the last solid will disappear. This point corresponds to point A* (x_s, T_1), *which is part of the melting-point curve.*

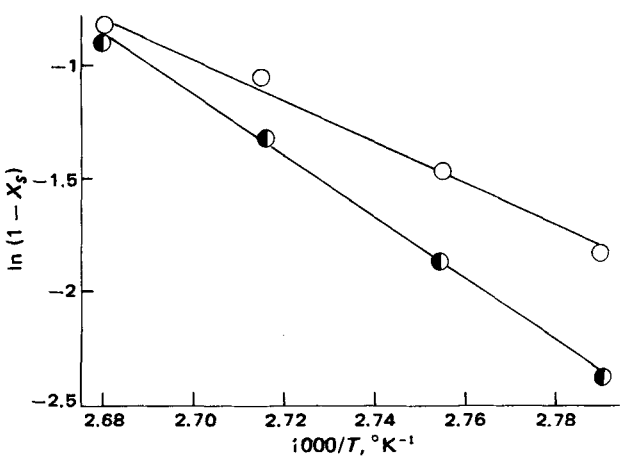

Figure 4—X_s *plotted as a function of 1000/*T. *Key:* ○, n = *10; and* ◐, n = *8.*

Table III—Least-Squares Fit Data According to Eq. 3.

n	Temperature	A	C	D	k_s, 10^4 hr^{-1}	R
8	85°	18.904	0.00858	0.00009	4.5	0.994
8	90°	10.973	0.0160	0.00008	14.6	0.992
8	95°	14.021	0.0435	0.00009	31.0	0.991
8	100°	12.579	0.106	0.00008	83.9	0.994
10	85°	20.289	0.00758	0.00002	3.7	0.990
10	90°	22.716	0.0283	0.00007	12.5	0.991
10	95°	18.814	0.0438	0.00008	23.3	0.992
10	100°	23.188	0.150	0.00008	64.5	0.994
12	85°	62.094	0.00915	0.00005	3.5	0.990
12	90°	39.795	0.0402	0.00007	10.1	0.992
12	95°	41.035	0.07842	0.00009	19.1	0.993
12	100°	47.860	0.245	0.00007	51.2	0.990
14	85°	22.456	0.00679	0.00007	3.0	0.997
14	90°	72.127	0.05965	0.00006	8.3	0.998
14	95°	123.577	0.1661	0.00007	13.4	0.992
14	100°	175.312	0.556	−0.00010	31.7	0.990
16	85°	30.196	0.00835	0.00004	2.8	0.990
16	90°	48.866	0.0460	0.00009	9.4	0.993
16	95°	42.389	0.0859	−0.00004	20.3	0.992
16	100°	54.795	0.358	0.0000	65.4	0.997
18	85°	24.460	0.00859	0.00007	3.5	0.998
18	90°	71.224	0.0453	0.00009	6.4	0.999
18	95°	51.261	0.0726	0.00009	14.2	0.998
18	100°	77.328	0.476	−0.00008	61.6	0.997

[a] n = alkyl lengths.

"proven"; it is simply established that the data generated do not conflict with it. Therefore, it is prudent to check the adherance in as many ways as possible to guarantee that the model is self-consistent.

It is obvious that the values of t_s and X_s are important, and some elaboration on this point will be made prior to testing the remaining points regarding Model C. If one considers a eutectic diagram (*e.g.*, Fig. 3), then it is obvious that at a given temperature, T_1, the point (X_s, T_1) is part of the melting-point curve, provided the two compounds, RCOOH and RH, form a simple melting-point diagram to the left of the eutectic point without solid solution formation.

The left eutectic diagrams, constructed from T *versus* X_s data, are given in Table II. The heat of fusion of RCOOH should be obtainable from these curves since:

$$\ln(1 - X_s) = \frac{(-\Delta H_f)(T_0 - T_s)}{RT_0T_s}$$

$$= (-\Delta H_f/R)[(1/T_s) - (1/T_0)] \quad \text{(Eq. 8)}$$

where T_0 is the melting point of RCOOH and T is the temperature corresponding to the particular X_s in consideration; R is the gas constant (8.3143 J mole^{-1} degree^{-1}). Examples of data plotted according to Eq. 8 are shown in Fig. 4. Least-squares fit parameters are shown on the bottom of Table II. The ΔH_f value is obtained by multiplying the slope by −8.31, and T_0 is minus the slope divided by the intercept. It should correspond to the melting point and, except for n = 8, this correlation is reasonably good.

The ΔH_f values obtained in this fashion are shown in Table I to enable comparison with data to be developed later. When differential thermal analysis (DTA) is applied, a ΔH value is obtained that is the heat of fusion for stable compounds. It is derived from the area under the endotherm. For compounds that decompose below their melting point, however, the ΔH value obtained from this area is the difference between the heat absorbed (ΔH_f) due to melting and the heat evolved (q) due to the reaction, *i.e.*:

$$\Delta H_{DTA} = \Delta H_f - q \quad \text{(Eq. 9)}$$

Therefore, the enthalpy of reaction ($-q$) can be deduced, and values of ΔH_{DTA} and q are listed in Table I. There were cases (n = 10 and n = 16) where the reaction taking place concurrent with or before melting made the thermograms so poorly reproducible that they are not reported here. The values for q should be viewed in this light as well. For n = 8, the melting point obtained from the kinetic data (Eq. 8) differs from that obtained by differential thermal analysis by several degrees. However, the latter is questionable rather than the former. The values of ΔH_f and q are not germane to the further development; they are included here simply for completeness and to indicate that ancillary values obtained in the study did not conflict with the proposed model.

As an example of the fits obtained *via* Eq. 3, the data shown by direct plotting in Fig. 1 were transposed *via* Eq. 3 and are shown in Fig. 5. The fit is good. Least-squares fit parameters obtained by iteration of Model A for all of the data are shown in Table III in the form:

$$\ln(1 + Ax) = Ct + D \quad \text{(Eq. 10)}$$

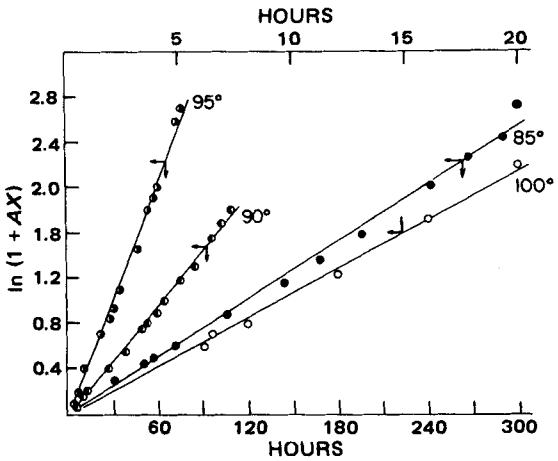

Figure 5—*Data from Fig. 1 plotted according to Eq. 3. Key:* ●, *85°;* ◐, *90°;* ◑, *95°; and* ○, *100°. Note dual scales.*

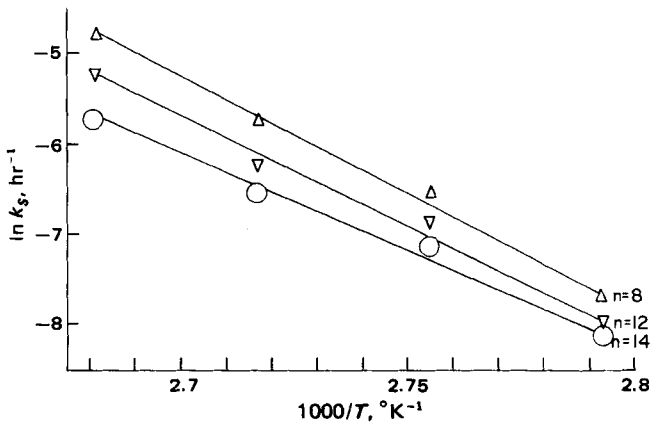

Figure 6—*Arrhenius plot of* k_s *(hr*$^{-1}$*). For graphical clarity, only* n = *8 (*△*),* n = *12 (*▽*), and* n = *14 (*○*) are shown.*

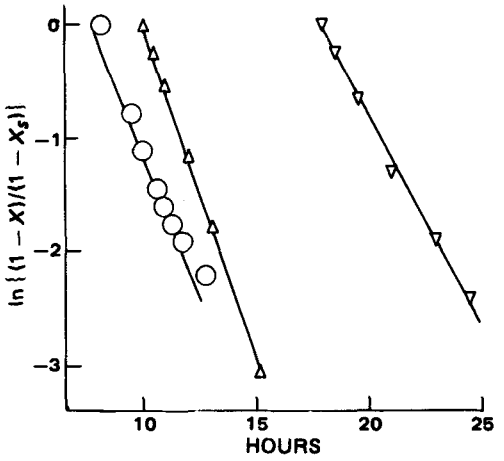

Figure 7—*First-order kinetics after the point where complete liquefaction has occurred. Key:* ▽, n = *10;* ○, n = *14; and* △, n = *16 (all at 100°).*

It is noted from the table that the D values are small (<0.0001) at the same time as R, the correlation coefficient, is high (never <0.99). Hence, C becomes synonymous with α in Eq. 3, allowing calculation of k_s *via* Eq. 4. The values of k_s obtained in this fashion are shown in Table III.

The temperature dependence of the k_s values is, according to the Arrhenius equation:

$$\ln k_s = -(E_a/R)(1/T) + \ln Z \qquad \text{(Eq. 11)}$$

where E_a is the activation energy and Z is a preexponential factor. This is exemplified in Fig. 6 (linearity is obvious upon visual inspection). Least-squares fit parameters are shown in Table IV, and the high correlation coefficients are indicative of the good fits.

As mentioned, the data in Table III ($A = \alpha/k_s$ and $C = \alpha$) in conjunction with the values from Table II [$S = (1 - X_s)/X_s$] will allow calculation of the decomposition rate in solution, k_l hr^{-1}. The parts of the curves beyond t_s can be used directly to calculate the first-order decomposition rate of RCOOH in solution in RH. An example is shown in Fig. 7; the linearity is graphically obvious, supporting the assumption of first-order kinetics in solution, *i.e.*, confirming Eq. 7. The reproducibility is fair at best (±10% for the rate constants). The rate constants obtained in this fashion are denoted simply k (Table V). The correlation coefficients confirm the visually observed linearity.

If the proposed model is correct, then k and k_l should be identical. They were plotted in linear fashion (Fig. 8); again, the linearity with a zero intercept is implied by:

$$k = A_1 k + B_1 \qquad \text{(Eq. 12)}$$

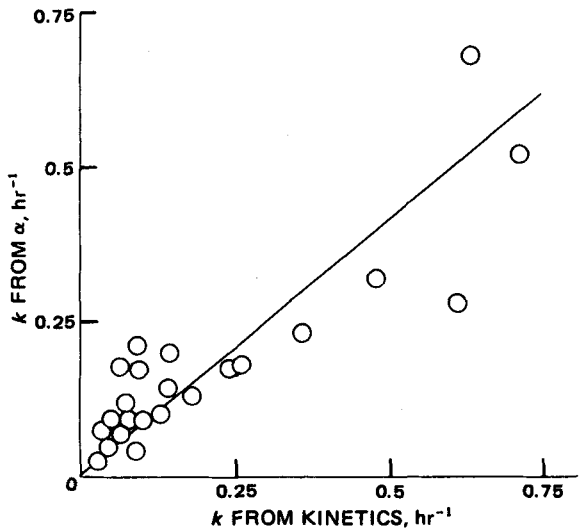

Figure 8—*Solution decomposition rate constants* (k_l) *derived from* α *as a function of solution decomposition rate constants* (k) *found experimentally.*

Table IV—Arrhenius Parameters for the Alkoxyfuroic Acids.

n^a	$10^{-5} E_a$, J/mole	Z
8	2.2	$3.69\ 10^{27}$
10	2.0	$2.62\ 10^{26}$
12	1.9	$5.09\ 10^{24}$
14	1.7	$9.9\ 10^{20}$
16	2.3	$3.8\ 10^{29}$
18	2.1	$6.78\ 10^{26}$

[a] n = alkyl length.

Table V—Solution Decomposition Rate Constants (Hour^{-1}) for the Alkoxyfuranoic Acids (RCOOH) in Solution in RH as a Function of Reciprocal Temperature Eq. 11

n^a	Correlation Coefficient, R^2	Intercept (ln Z')	Slope ($-E_a/R$)	E_a, kJ/mole	Z
8	0.972	22.89	−9,113	76	0.87×10^{10}
10	0.984	51.01	−19,513	162	1.42×10^{22}
12	0.969	50.15	−19,083	159	6.02×10^{21}
14	0.933	55.78	−20,903	174	1.68×10^{24}
16	0.925	55.66	−21,006	176	1.49×10^{24}
18	0.911	50.96	−19,239	160	1.35×10^{22}

[a] n = alkyl length.

where A_1 should be unity and B_1 should be zero. The least-squares fit values in Fig. 8 are $A_1 = 0.83 \pm 0.22$ and $B_1 = 0.17 \pm 0.25$, so the figure does not contradict the proposed model. The overall correlation coefficient is 0.975.

The k_l or k values should be treatable by the Arrhenius equation (Fig. 9). The least-squares fit parameters for these relations are shown in Table V.

Pothisiri and Carstensen (4) suggested that the temperature at which $k_l = k_s$ (T_i) is related to the melting point (T_m) in log–log fashion. Data from the present study are pooled with data from Ref. 4, in Fig. 10, and the correlation seems to hold with the alkoxyfuroic acids as well as previously reported compounds. Since the furoic acids have melting temperatures close to one another, they have been averaged, as has T_i (Fig. 10). With the small number of compounds at present, this is, at best, a rank-order correlation.

An attempt was made to correlate the kinetic parameters with substituent properties (chain length) in Fig. 11. Both E_a and Z decreased

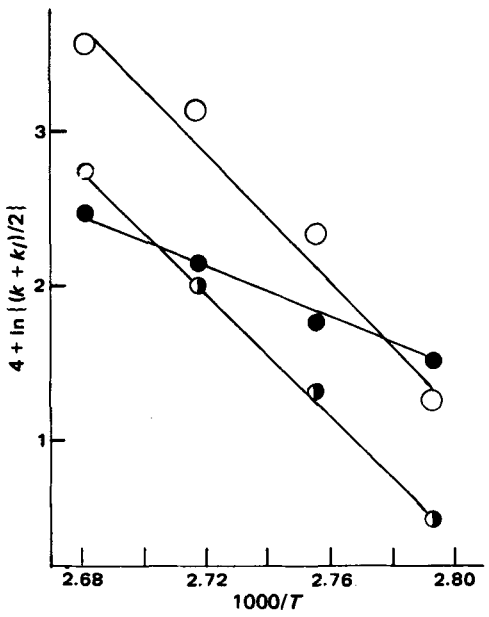

Figure 9—*Logarithm of the solution decomposition rate constants of RCOOH in solution in RH plotted as a function of 1000/T (°K^{-1}). Key:* ●, n = *8;* ◑, n = *10; and* ○, n = *14. The remainder are left out for graphical clarity.*

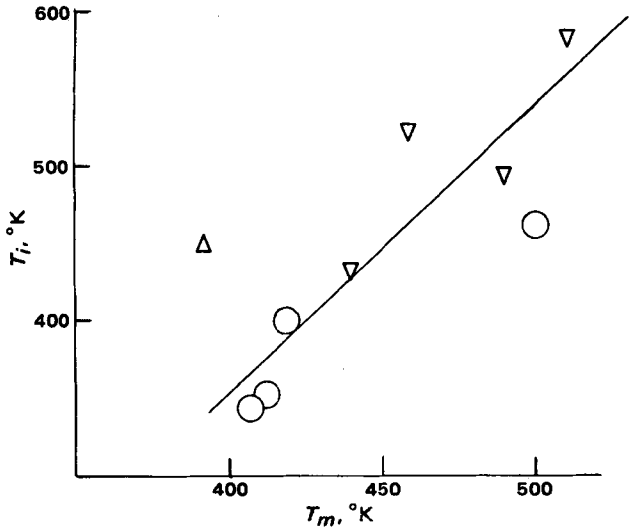

Figure 10—*Data from Refs. 3 (∇) and 4 (○) plotted together with the average* T_m *and* T_i *values (△) from this study. (Average* T_m *= 394 ± 4 °K and, average* T_i *= 450 ± 50 °K.)*

with increasing chain length up to n = 14, after which there was an upward break in the curve. This discontinuity did not exist in other properties of the series (vapor pressures, densities, and enthalpies of fusion and reaction). No explanation is offered for this break at present.

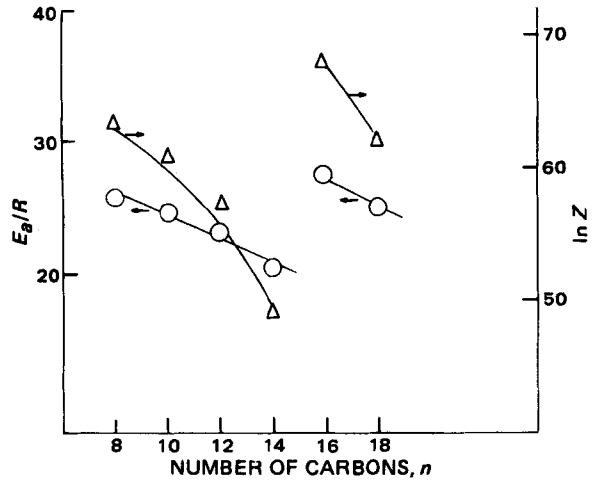

Figure 11—E_a/R *and ln Z from Eq. 11 (Table IV) plotted* versus n. *The values for* n = *14 are slightly (4%) lower than previously reported (6) due to increased precision in this study (multiple runs).*

The effect of particle size was estimated by micronizing a sample (n = 14). At 85°, this sample had a value of $k_s = 3.3 \times 10^{-4}$/hr as opposed to 3.3×10^{-4}/hr for a nonmicronized sample; therefore the effect of particle size was not pronounced. All samples tested were not milled, *i.e.*, were in the recrystallized state, and had surface areas, measured by nitrogen adsorption, of ~1 m^2/g.

A final note on reproducibility is in order. Data were duplicated with parameter values obtained from 10 sets that differed by no more than 5%. The effect of the use of a mercury manometer as contrasted to the use of break-seal tubes was also tested (in five cases) with duplication within the previously mentioned error.

Therefore, it is fairly conclusive that the alkoxyfuroic acids decompose as shown in Scheme II, and solid and liquid decomposition rate constants have been established. The liquefaction characteristics are in accordance with what would be expected from melting-point diagrams with a reasonable correlation. Energy of activation is a function of chain length, as is the preexponential factor. There is a break in this correlation curve at n = 14/16. The isokinetic temperature (T_i) falls fairly well on the correlation line established for other compounds.

REFERENCES

(1) E. G. Prout and F. C. Tompkins, *Trans. Faraday Soc.*, **40,** 488 (1944).

(2) C. E. H. Bawn, in "Chemistry of the Solid State," W. E. Garner, Ed., Butterworths, London, England, 1955, p. 254.

(3) J. T. Carstensen and M. N. Musa, *J. Pharm. Sci.*, **61,** 1112 (1972).

(4) P. Pothisiri and J. T. Carstensen, *ibid.*, **64,** 1931 (1975).

(5) J. T. Carstensen and P. Pothisiri, *ibid.*, **64,** 37 (1975).

(6) J. T. Carstensen and R. C. Kothari, *ibid.*, **69,** 123 (1980).

(7) R. A. Parker, T. Karyia, J. M. Grisar, and V. Petrow, *J. Med. Chem.*, **20,** 781 (1977).

(8) R. M. Whittaker, *Rec. Trav. Chim.*, **52,** 352 (1933).

(9) M. Knudsen, *Ann. Phys.*, **28,** 999 (1909).

(10) *Ibid.*, **29,** 179 (1909).

(11) M. J. Pikal and A. L. Lukes, *J. Pharm. Sci.*, **65,** 1269 (1976).

(12) *Ibid.*, **65,** 1278 (1976).

(13) M. Davies and B. Kybett, *Trans. Faraday Soc.*, **61,** 1608 (1963).

(14) L. VanCampen, G. Zografi, and J. T. Carstensen, *Int. J. Pharm.*, **5,** 1 (1980).

ACKNOWLEDGMENTS

Presented in part at the APhA Academy of Pharmaceutical Sciences, San Antonio meeting, November 1980.

Abstracted in part from a thesis submitted by R. Kothari to the University of Wisconsin in partial fulfillment of the Doctor of Philosophy degree requirements.

Supported in part by a research grant from Hoffmann–La Roche, Nutley, NJ 07110.

The authors thank Dr. J. Sheridan, Hoffmann–La Roche, Nutley, N.J., and Dr. M. A. Zoglio and Dr. R. A. Parker, Merrell-National Laboratories, Cincinnati, Ohio, for technical assistance.